

Detecting Obscured AGN in the Distant Universe with *Spitzer*

J. L. Donley,¹ G. H. Rieke,¹ P. G. Pérez-González,^{1,2} J. R. Rigby,¹ A. Alonso-Herrero³

Abstract.

We present the results of a *Spitzer* search for obscured AGN in the *Chandra* Deep Field-North, using both radio-excess and mid-infrared power-law selection. AGN selected via the former technique tend to lie at $z \sim 1$, have SEDs dominated by the $1.6 \mu\text{m}$ stellar bump, and have Seyfert-like X-ray luminosities (when detected in the X-ray). In contrast, the IRAC ($3.6\text{-}8.0 \mu\text{m}$) power-law selected AGN lie at higher redshifts of $z \sim 2$, and comprise a significant fraction of the most X-ray luminous AGN in the CDF-N. While there is almost no overlap in the AGN samples selected via these two methods, their X-ray detection fractions are very similar. Only 40% and 55% of the radio-excess and power-law samples are detected in the 2 Ms X-ray catalog, respectively. The majority of the AGN selected via both methods are consistent with being obscured ($N_{\text{H}} > 10^{22} \text{ cm}^{-2}$), but not Compton-thick ($N_{\text{H}} > 10^{24} \text{ cm}^{-2}$), although Compton-thick candidates exist in both samples. We place an upper limit of $\leq 82\%$ (or $\leq 4 : 1$) on the obscured fraction of the power-law sample, consistent with predictions from the cosmic X-ray background. The sources selected via the power-law criteria comprise a subset of AGN selected via other IRAC color-color cuts. While smaller in number than the color-selected samples in the deep fields, the power-law sample suffers from less contamination by star-forming galaxies.

1. Introduction

Defining complete samples of AGN, both locally and in the distant cosmological fields, has been a major ongoing goal of AGN research. Hard X-ray selection is generally considered the best way to detect both relatively uncontaminated and complete samples of AGN. At high column densities, however, the dust and gas surrounding the central engine (in combination with that located in the host galaxy) are capable of hiding virtually all accessible AGN tracers. Therefore, while the overall resolved fraction of the cosmic X-ray background (CXRB) is high, it drops with increasing energy to 60% at 6-8 keV and to 50% at $> 8 \text{ keV}$ (Worsley et al. 2004, 2005). Population synthesis models of the CXRB therefore predict a significant population of heavily obscured AGN not detected in the

¹Steward Observatory, University of Arizona, 933 North Cherry Avenue, Tucson, AZ 85721; jdonley@as.arizona.edu

²Departamento de Astrofísica y CC. de la Atmósfera, Facultad de CC. Físicas, Universidad Complutense de Madrid, 28040 Madrid, Spain

³Departamento de Astrofísica Molecular e Infrarroja, Instituto de Estructura de la Materia, CSIC, E-28006 Madrid, Spain

deepest X-ray fields. For instance, Treister et al. (2004) predict that current X-ray catalogs are 25% incomplete at $N_H = 10^{23} \text{ cm}^{-2}$ and 70% incomplete at $N_H = 10^{24} \text{ cm}^{-2}$.

Numerous attempts have been made to detect this population of heavily obscured AGN, many of which have focused on the mid-infrared (MIR) emission where the obscured radiation is re-emitted or on combinations of MIR and multi-wavelength data. We focus here on two selection techniques independent of the optical and X-ray properties of the AGN: radio-excess and MIR power-law selection. The former selects AGN whose radio emission far exceeds that of the radio-infrared correlation for star-forming galaxies, whereas the latter selects AGN whose IRAC SEDs exhibit the characteristic power-law emission expected of luminous AGN (e.g. Elvis et al. 1994). By focusing on the infrared and radio, wavebands where dust obscuration is minimal, we can select both unobscured AGN as well as heavily obscured AGN likely to be missed in the UV, optical, and soft X-ray bands.

To test the X-ray properties of the *Spitzer*-selected AGN samples, we focus on the CDF-N, the deepest X-ray field observed to date. *Spitzer* MIPS and IRAC images with exposures of 1400 s and 500 s, respectively, cover the full area of the *Chandra* 2 Ms field, as does the deep 1.4 GHz radio data of Richards (2000). Optical and near-infrared imaging and photometry are available from the GOODS dataset (Giavalisco et al. 2004) as well as from the data of Capak et al. (2004) (*UBVRIz'HK'*). We assume a cosmology of $(\Omega_m, \Omega_\Lambda, H_0) = (0.3, 0.7, 72 \text{ km s}^{-1} \text{ Mpc}^{-1})$.

2. Radio-excess Sample

We use the well-known radio-infrared relation of star-forming galaxies and radio-quiet AGN, to select a sample of radio-excess AGN. Appleton et al. (2004) define $q = \log(f_{24 \mu\text{m}}/f_{1.4 \text{ GHz}})$. For star-forming galaxies, q is tightly constrained out to $z \sim 1$: $q = 0.94 \pm 0.23$ after K-correction (Appleton et al. 2004). Galaxies with values of q well below this range (strong radio with respect to 24 μm emission) are unlikely to be dominated by star formation and instead are radio-emitting AGN (e.g. Condon et al. 1995). We therefore set a selection threshold of $q < 0$ to classify a galaxy as probably having an AGN and require a *Chandra* exposure of > 1 Ms to provide high X-ray sensitivity. This selection identifies 27 radio-excess AGN in the CDFN (Donley et al. 2005).

The radio-excess AGN lie at the typical redshift of X-ray sources in the CDF-N, $z \sim 1$, and (when detected in the X-ray) tend to have X-ray luminosities typical of Seyfert galaxies and SEDs dominated by the 1.6 μm stellar bump. Approximately 60% of these radio-excess AGN, however, are X-ray undetected in the 2 Ms *Chandra* catalog, even at exposures of ≥ 1 Ms; 25% lack even 2σ X-ray detections. The absorbing columns to the faint X-ray-detected objects are $10^{22} \text{ cm}^{-2} < N_H < 10^{24} \text{ cm}^{-2}$, i.e., they are obscured but unlikely to be Compton thick. Of the 9 AGN that are either X-ray non-detected or are too close to a known X-ray source to search for weak X-ray emission, we estimate that 6 could be Compton thick. This corresponds to 22% of our sample and is consistent with predictions from the X-ray background.

3. MIR Power-law Sample

In the MIR, luminous AGN can often be distinguished by their characteristic power-law emission, which extends from the infrared to the ultraviolet (e.g. Neugebauer et al. 1979; Elvis et al. 1994). This emission is not necessarily due to a single source, but can arise from the combination of non-thermal nuclear emission and thermal emission from various nuclear dust components (e.g. Rieke & Lebofsky 1981).

Alonso-Herrero et al. (2006) selected a sample of 92 such sources in the CDF-S, 70% of which are hyper-luminous infrared galaxies (HyperLIRGs, $\log L_{\text{IR}}(L_{\odot}) > 13$) or ultra-luminous infrared galaxies (ULIRGs, $\log L_{\text{IR}}(L_{\odot}) > 12$). Nearly half (47%) of their power-law sample were undetected in X-rays at exposures of up to 1 Ms. We use a selection similar to that of Alonso-Herrero et al. (2006) to identify a sample of 62 high S/N , red ($\alpha \leq -0.5$, where $f_{\nu} \propto \nu^{\alpha}$) IRAC power-law galaxies in the 2 Ms CDF-N (Donley et al. 2007).

3.1. X-ray Properties

Of the 62 power-law galaxies, only 34 (55%) have X-ray counterparts in the 2 Ms CDF-N X-ray catalog (Alexander et al. 2003), consistent with the findings of Alonso-Herrero et al. (2006), although 85% show evidence for X-ray emission at the $\geq 2.5\sigma$ detection level. While the power-law galaxies comprise only $\sim 20\%$ of the X-ray and MIR-detected AGN in the CDF-N, they make up a significant fraction of the high redshift ($z \sim 2$) and high luminosity X-ray AGN sample, as is demonstrated in Fig. 1. This is not surprising, as the power-law selection requires the AGN to be energetically dominant, and therefore preferentially selects the most luminous AGN. To illustrate the effect of X-ray luminosity on the AGN contribution to the optical through MIR continuum, we also plot in Fig. 1 the median rest-frame optical-MIR SEDs of the X-ray-detected members of the comparison sample, as a function of X-ray luminosity. The comparison sample consists of the 1420 IRAC sources in the CDF-N that meet our S/N and X-ray exposure cuts. Low-luminosity X-ray sources are dominated by the stellar bump in the optical-NIR bands (e.g. Alonso-Herrero et al. 2004). The strength of this feature decreases with increasing X-ray luminosity, and disappears almost entirely at luminosities of $\log L_{\text{x}}(\text{ergs s}^{-1}) > 44$, where the SED takes on the characteristic power-law shape.

3.2. Obscuration

The obscured fraction ($N_{\text{H}} > 10^{22} \text{ cm}^{-2}$) of the X-ray-detected power-law galaxies is $\sim 68\%$, in agreement with that of Ueda et al. (2003) for AGN at similar redshifts. If we consider only those power-law galaxies in the X-ray catalog, we therefore derive an obscured to unobscured ratio of $\sim 2:1$. Adding the 10 weakly-detected power-law galaxies, all of which are likely to be obscured, we calculate an obscured fraction of $\sim 75\%$. If we further include the power-law galaxies not detected in X-rays, assuming that all are obscured, the maximum obscured ratio of power-law galaxies rises to $< 4:1$ - $5:1$ (82%).

Power-law galaxies detected to high S/N in the IRAC bands account for at most $\sim 20 - 30\%$ of both the MIR-detected AGN and the MIR-detected obscured AGN predicted by the X-ray luminosity function synthesis models of

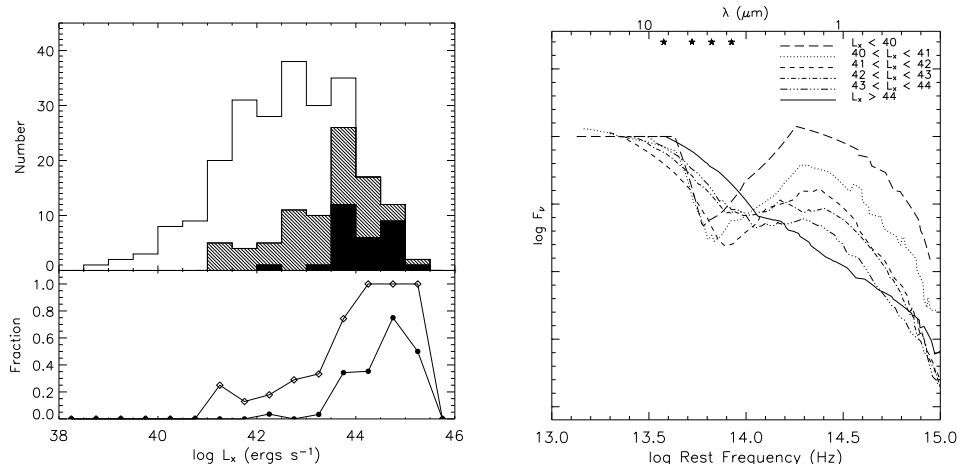


Figure 1. Left: X-ray luminosity distributions of X-ray-detected IRAC sources (unshaded histogram), the power-law sample (filled histogram) and the sample of AGN selected by the Lacy et al. (2004) color criteria (lightly shaded). The lower panel gives the fraction of the X-ray sources that meet the power-law (filled circles) or Lacy et al. (open diamonds) criteria. Right: Median rest-frame SEDs of the X-ray-detected IRAC sources, as a function of observed 0.5-8 keV luminosity (in units of ergs s^{-1}). Stars indicate the wavelengths of the four IRAC bands.

Treister et al. (2006) down to $24 \mu\text{m}$ flux densities of $80 \mu\text{Jy}$. The majority of obscured AGN should therefore have SEDs dominated by the host galaxy, or red power-law SEDs that fall below the IRAC detection limit.

3.3. Comparison to IRAC Color-Selection

We plot in Fig. 2 the position of the power-law galaxies with respect to the IRAC AGN color cuts of Lacy et al. (2004) and Stern et al. (2005), designed for relatively shallow surveys. All of the power-law galaxies lie within both the Lacy et al. and Stern et al. color regions, and as such, they comprise a subset of the color-selected MIR sources. While the color-selected AGN samples in the CDF-N comprise a higher fraction of high-luminosity AGN than the power-law selected sample (see Fig. 1), they also appear to suffer from a higher degree of contamination from star-forming galaxies (see Table 1). This is not surprising, given the behavior of the star-forming and AGN templates shown in Fig. 2 (available in Donley et al. 2007). The star-forming templates enter the AGN selection regions at both low and high redshifts, whereas they fall outside of the more stringent power-law region at $z < 2.8$.

4. Summary

We present the results of a *Spitzer* search for AGN in the *Chandra* Deep Field-North. We focus on two selection techniques independent of the optical and X-ray properties of the sources. The first is radio-excess selection, in which we select sources whose radio emission far exceeds that of the radio-infrared

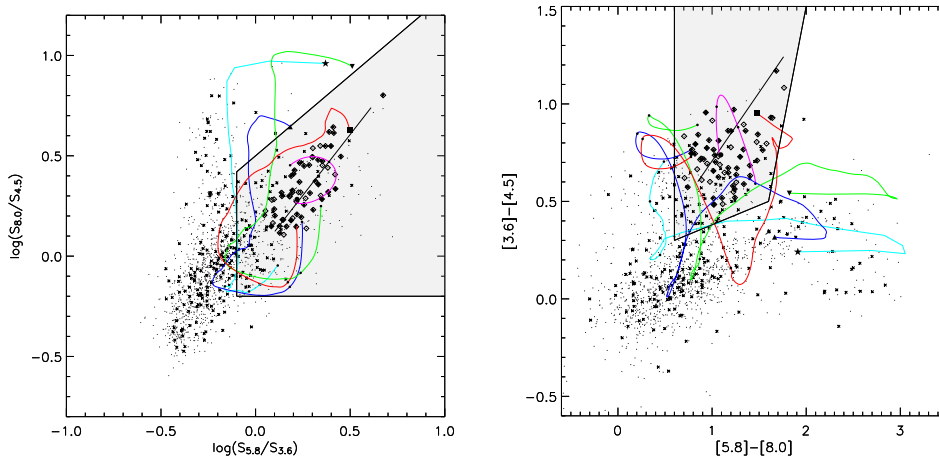


Figure 2. Location of CDF-N IRAC sources on the color-color diagram of Lacy et al. (2004, left) and Stern et al. (2005, right). Power-law galaxies are given by diamonds and X-ray sources are given by crosses. The 7 power-law galaxies that are X-ray non-detected to the 2.5σ level are shown as filled diamonds. Overplotted are the redshifted IRAC colors of a typical star-forming galaxy (Dale & Helou 2002, cyan star), the starburst-dominated ULIRGs Arp 220 (blue triangle) and IRAS 17208 (green upside down triangle), the ULIRG/Sey 2 Mrk 273 (red square) and the radio-quiet AGN SED from Elvis et al. (1994, magenta circle), where the indicated point represents the colors at $z = 0$, and small circles mark the colors at $z = 1, 2$, and 3 . The star-forming templates enter the color-selection regions at both low and high redshifts, but fall outside of the more stringent power-law region at $z < 2.8$.

Table 1. Properties of power-law and color-selected CDF-N samples

Selection Criteria	Power-law	Stern et al.	Lacy et al.
Number	62	216	393
Detected in X-rays	55%	38%	25%
Detected at $24\mu\text{m}$	>92%	83%	72%
$L_{1.4\text{GHz}} > 10^{24} \text{ W Hz}^{-1}$	88%	54%	49%
Quiescent Optical/X-ray Colors	$\geq 3\%$	$\geq 10\%$	$\geq 15\%$

correlation. In the CDF-N, we detect 27 radio-excess AGN. These sources tend to lie at $z \sim 1$ and have SEDs dominated by the $1.6 \mu\text{m}$ stellar bump. Only 40% are detected in the X-ray at exposures of $> 1 \text{ Ms}$, although 75% show signs of X-ray emission at the $> 2\sigma$ detection level. Those with X-ray counterparts have Seyfert-like X-ray luminosities. The majority of the radio-excess AGN are consistent with being obscured ($N_{\text{H}} > 10^{22} \text{ cm}^{-2}$), and 20% are potentially Compton-thick.

The second selection technique is MIR power-law selection, in which we select sources with red ($\alpha < -0.5$) IRAC power-law SEDs. The sources selected in this way tend to have higher redshifts ($z \sim 2$) and X-ray luminosities than the radio-excess sample. The IRAC power-law selection recovers a significant

fraction of the most X-ray luminous AGN in the CDF-N. Despite this, only 55% of the power-law galaxies are detected in the X-ray, with 15% remaining undetected down to the $> 2.5\sigma$ detection level. These X-ray detection fractions are similar to those of the radio-excess AGN, even though there is almost no overlap in the two samples. This suggests that a relatively low X-ray detection rate may be a common feature for AGN samples selected independently of their optical and X-ray properties, regardless of luminosity or redshift.

A study of the intrinsic obscuration of the power-law galaxies suggests that as many as 82% (4:1 - 5:1) are obscured. The number densities of these sources indicate that the power-law sample comprises only 20-30% of the MIPS-detected obscured AGN population. The remaining AGN are likely to have SEDs dominated by the host galaxy, like those of the radio-excess sample.

The power-law galaxies discussed here comprise a subset of AGN selected via the IRAC color-selection criteria of Lacy et al. (2004) and Stern et al. (2005). While larger in number than the power-law sample, the color-selected samples in the CDF-N appear to suffer from a higher degree of contamination from star-forming galaxies. By applying additional SED constraints to a color-selected sample, or by requiring either a 24 μm detection or AGN-like optical/X-ray colors, one can create both a more complete and reliable sample of MIR-selected AGN, even in the deepest astronomical fields. Doing so is crucial if we are to constrain the fraction of heavily obscured AGN in the distant universe and determine their contribution to the accretion history of the universe.

Acknowledgments. This work was supported by an NSF Graduate Research Fellowship and by NASA through contracts 960785 and 1255094, issued by JPL/California Institute of Technology.

References

- Alexander, D. M., et al. 2003, *AJ*, 126, 539
 Alonso-Herrero, A., et al. 2004, *ApJS*, 154, 155
 Alonso-Herrero, A., et al. 2006, *ApJ*, 640, 167
 Appleton, P. N., et al. 2004, *ApJS*, 154, 147
 Capak, P., et al. 2004, *AJ*, 127, 180
 Condon, J. J., Anderson, E., & Broderick, J. J. 1995, *AJ*, 109, 2318
 Dale, D. A., & Helou, G. 2002, *ApJ*, 576, 159
 Donley, J. L., Rieke, G. H., Rigby, J. R., & Pérez-González, P. G. 2005, *ApJ*, 634, 169
 Donley, J. L., Rieke, G. H., Pérez-González, P. G., Rigby, J. R., Alonso-Herrero, A., submitted to *ApJ*
 Elvis, M., et al. 1994, *ApJS*, 95, 1
 Giavalisco, M., et al. 2004, *ApJ*, 600, L93
 Lacy, M., et al. 2004, *ApJS*, 154, 166
 Neugebauer, G., Oke, J. B., Becklin, E. E., & Matthews, K. 1979, *ApJ*, 230, 79
 Richards, E. A. 2000, *ApJ*, 533, 611
 Rieke, G. H., & Lebofsky, M. J. 1981, *ApJ*, 250, 87
 Stern, D., et al. 2005, *ApJ*, 631, 163
 Treister, E., et al. 2004, *ApJ*, 616, 123
 Treister, E., et al. 2006, *ApJ*, 640, 603
 Ueda, Y., Akiyama, M., Ohta, K., & Miyaji, T. 2003, *ApJ*, 598, 886
 Worsley, M. A., Fabian, A. C., Barcons, X., Mateos, S., Hasinger, G., & Brunner, H. 2004, *MNRAS*, 352, L28
 Worsley, M. A., et al. 2005, *MNRAS*, 357, 1281